

Collision-Sensitive Spin Noise

Shiming Song,^{1,2,3} Min Jiang,^{1,2,3,*} Yushu Qin,^{1,2,3} Yu Tong,^{1,2,3} Wenzhe Zhang^{1,2,3},[✉] Xi Qin,^{1,2,3}
Ren-Bao Liu,⁴ and Xinhua Peng^{1,2,3,†}

¹*Hefei National Laboratory for Physical Sciences at the Microscale and Department of Modern Physics,
University of Science and Technology of China, Hefei 230026, China*

²*CAS Key Laboratory of Microscale Magnetic Resonance, University of Science and Technology of China, Hefei,
Anhui 230026, China*

³*Synergetic Innovation Center of Quantum Information and Quantum Physics, University of Science and
Technology of China, Hefei, Anhui 230026, China*

⁴*Department of Physics, Centre for Quantum Coherence, and The Hong Kong Institute of Quantum Information
Science and Technology, The Chinese University of Hong Kong, Shatin, New Territories, Hong Kong, China*

(Received 19 July 2021; revised 16 November 2021; accepted 22 November 2021; published 4 January 2022)

Collision phenomena are ubiquitous and highly useful in determining the microscopic structures and intermolecular interactions of atoms and molecules. The existing approaches are mostly based on atomic or molecular scatterings, which are hindered by the inconvenience of using ultrahigh vacuum and low-temperature systems. Here we demonstrate a spin-noise spectroscopic approach by measuring optical polarization rotation noise of the probe light with simple apparatus and ambient conditions. Our approach features tens of gigahertz bandwidth and one part-per-million resolution, outperforming previous spin-noise techniques. Enabled by the technique, we observe the collision-sensitive spin noise of alkali atoms, and precisely determine key collision parameters, such as collision diameter, well depth, and dominant interaction type. Our work provides a tool to study a broad range of collision phenomena under ambient conditions.

DOI: 10.1103/PhysRevApplied.17.L011001

Introduction.—Collisions are ubiquitous in physics, chemistry, and thermodynamics. The analysis of collision phenomena plays a role in determining the microscopic structures [1,2], interactions [3–5], and energy stability [6–11] of atoms and molecules. Collision phenomena have been studied by a large variety of techniques, such as scattering experiments [1,2,4], absorption spectra [3,5], and nuclear magnetic resonance [12]. Among these techniques, scattering experiments using atomic or molecular beams are mostly used. However, such scattering methods usually require a high vacuum degree less than 10^{-3} torr and low temperature as low as tens of kelvin [4], which place severe limits in their realistic applications. It remains challenging to, for example, study collisions under relatively high pressures, where projectile atoms or molecules collide with target gases multiple times. This increases the complexity of collision processes and introduces additional experimental errors. Besides, such approaches are not suitable for *in situ* measuring collisions inside of encapsulated quantum devices, which have many useful applications in atomic vapor magnetometers [13–17] and electrometers [18]. Therefore, it is highly desirable to develop techniques

that can investigate collision phenomena in wide-ranging experimental conditions.

Colliding particles may exhibit alternative properties, such as energy-level shifts [6–8,11,19,20], collision-induced absorption [3,5], and interatomic entanglement [21,22]. Recently, collisions between alkali atoms and inert atoms or molecules have attracted considerable attention in the areas of frequency standards [6], metrology [13–18], and quantum information [21,22]. Direct measurement of spin noise in thermodynamic equilibrium by optical rotation is becoming a mainstream approach for nonperturbative studies of energy structures [23–32], spatial properties [33], and correlated states [34–37] in diverse systems, such as alkali atomic vapors [23,24]. Collision phenomena can be analyzed by measuring the collision-sensitive spin noise whose frequency is altered due to collisions. Specifically, collisions can be investigated by measuring energy spectra of the collision-sensitive spin noise. However, when it is used to measure collision-induced energy shifts, this places high demands both for measurement bandwidth and for spectral resolution. Specifically, direct observation of collisional shifts of Zeeman sublevels is much more difficult than that of interhyperfine levels. For example, shifts of Zeeman sublevels at a magnetic field of 1 G are 7 orders of magnitude smaller than that of the interhyperfine levels [7]. Accordingly, to detect collisional shifts of

*dxjm@ustc.edu.cn

†xhpeng@ustc.edu.cn

microwave interhyperfine levels, the gigahertz bandwidth is required. The other requirement is high resolution, because collisional shifts are still only 1–10 parts per million for interhyperfine levels [6,8]. Unfortunately, existing spin-noise techniques based on the optical-rotation approach suffer from a trade-off between bandwidth and resolution [31,38,39]. The best resolution is only several hundred kilohertz at gigahertz frequency range [39].

In this Letter, we demonstrate a realization of measuring collision phenomena by developing and applying spin-noise spectroscopy that has gigahertz bandwidth and part-per-million resolution. The collision-sensitive spin noise arising from interhyperfine levels is detected by optical rotation. Noise spectra are analyzed to reveal collisional energy shifts. We apply our technique to *in situ* measure spin noise of alkali atoms colliding with a variety of inert atoms and molecules, and obtain key collision parameters, including the collision diameter, the well depth, and the dominant interaction type. The results are in good agreement with theory. Our method avoids extra heating effects and atom loss caused by pumping [40], and provides a promising way for nonperturbatively studying cold and ultracold collisions [34,35].

Spin noise as a probe of collision.—Consider the case of binary collision, where two particles interact through an effective potential depending on their relative distance. For an alkali atom colliding with an inert atom or molecule, the wave function of the valence electron is perturbed and thus energy levels (e.g., optical energy levels [20,41] and hyperfine energy levels [6–8,19]) undergo shifts. According to the statistical theorem, the mean energy shift of the alkali atomic ensemble equals the statistical mean of all perturbations under every general condition [6,19]. Therefore, the collisional frequency shift can be expressed as (here we assume $\hbar = 1$) [6]

$$\nu_{\text{shift}} = 4\pi n \int \delta E(r) e^{-U(r)/k_B T} r^2 dr, \quad (1)$$

where r is the distance between the collision pair, $U(r)$ is the effective intermolecular potential, $\delta E(r)$ is the energy perturbation on the alkali atom from collisions, n is the density of inert atoms or molecules, and T is the temperature.

The intermolecular potential and the energy perturbation can be simplified as the summation of a long-range van der Waals attraction and a short-range Pauli repulsion, such as the Lennard-Jones potential [42]

$$\begin{aligned} U(r) &= 4\epsilon_1[(\sigma_1/r)^{12} - (\sigma_1/r)^6], \\ \delta E(r) &= 4\epsilon_2[(\sigma_2/r)^{12} - (\sigma_2/r)^6]. \end{aligned} \quad (2)$$

Here σ_1 is the node where the potential $U(r)$ is zero, and is called the collision diameter. ϵ_1 is the well depth.

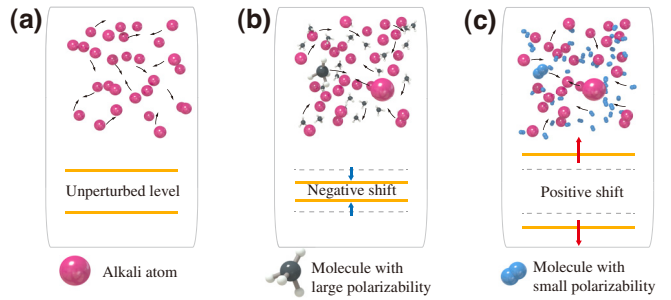


FIG. 1. Collision-induced energy shifts. (a) Unperturbed energy level of alkali atoms, such as rubidium atoms. (b) Negative energy shift of alkali atoms colliding with atoms or molecules with large electric polarizability, such as Rb-CH₄ collision. (c) Positive energy shift of alkali atoms colliding with atoms or molecules with small electric polarizability, such as Rb-N₂ collision.

Similarly, $\delta E(r)$ is zero at $r = \sigma_2$ and its minimum is $-\epsilon_2$. As an example of collisional shifts shown in Fig. 1, the hyperfine splitting of alkali atoms arises from the Fermi-contact interaction of the valence electron and the nucleus [43], and is proportional to the valence electron density at nucleus [8]. Figure 1(a) shows such an alkali ensemble and corresponding unperturbed energy levels (we adopt two of these levels as an example). Here we neglect shifts induced by collisions between alkali atoms themselves, which are usually less than 10⁻⁶ Hz [9]. The attractive force tends to pull the valence electron away from the nucleus and therefore reduces the hyperfine interaction while the short-range repulsive force increases the interaction. As shown in Fig. 1(b), an inert atom or molecule with relatively large electric polarizability, such as CH₄, usually has a dominant van der Waals attractive force, which therefore causes negative shifts of hyperfine interaction [8]. Whereas inert atoms or molecules with relatively small electric polarizability as shown in Fig. 1(c), such as N₂, cause positive shifts [8].

We now consider how to use the spin-noise technique to measure collisions in a vapor cell. The vapor cell comprises a natural abundance of rubidium atoms and other colliding atoms or molecules to be studied. As depicted in Fig. 2, linearly polarized light is focused through the cell, the longitudinal spin polarization of the atoms causes rotation of the light polarization. As the spin polarization fluctuates randomly, the polarization rotation is in turn fluctuating. The transient rotation can be measured with a high-bandwidth photodiode and analyzed by a home-built field-programmable gate-array- (FPGA) based spectrum analyzer [44]. According to the fluctuation-dissipation theorem [31,45,46], collision-sensitive spin-noise spectra can reveal spin properties of colliding alkali atoms, such as energy levels [31,46] and their collisional shifts, and spin dephasing rates [45]. This establishes a bridge between

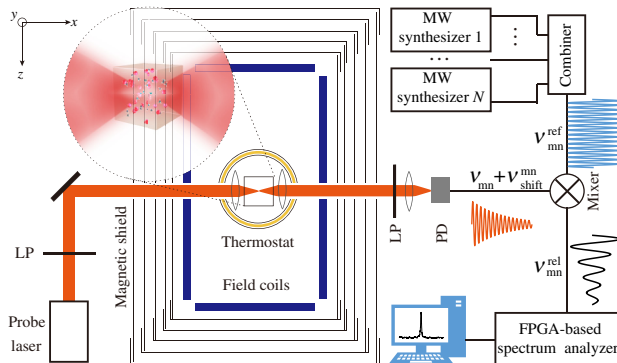


FIG. 2. Schematic of measuring collision-sensitive spin noise. A vapor cell containing a natural abundance of Rb atoms and inert atoms or molecules is placed within an oven, and shielded inside a five-layer μ -metal shield. A 14-mW linearly probe laser is detuned 100 GHz from the Rb D2 optical transition and focused through the cell with about $230\ \mu\text{m}$ diameter. Intrinsic fluctuations of Rb spins $\delta S_x(t)$ impart small rotation fluctuations $\delta\theta \propto \delta S_x(t)$ on the laser [24], detected by a linear polarizer (LP) and a photodetector (PD) with a bandwidth of 12.5 GHz. The high-frequency raw signals are then mixed with an array of microwave (MW) synthesizers to generate low-frequency signals (see text). At last, down-converted signals are sent to a home-built FPGA-based spectrum analyzer [44].

collisions and the spin-noise spectrum

$$S_\alpha(\nu) = \sum_{m,n} (\rho_m + \rho_n) |\langle m | \mathbf{S} \cdot \hat{\alpha} | n \rangle|^2 \times \frac{\gamma_{mn}}{(\nu - \nu_{mn} - \nu_{\text{shift}}^{mn})^2 + \gamma_{mn}^2}, \quad (3)$$

where ρ_m is the occupation factor of level m with eigenfrequency ν_m . $\hat{\alpha}$ is the unit vector along the probe laser propagation direction. $\nu_{mn} + \nu_{\text{shift}}^{mn} = \nu_m - \nu_n + \nu_{\text{shift}}^{mn}$ is the transition frequency of the alkali atom, and is usually on the order of 1 GHz and 1 MHz for hyperfine splittings and Zeeman splittings, respectively. The spin dephasing rate γ_{mn} , which is usually on the order of 1 kHz, determines the spectral resolution.

However, current spin-noise techniques are not suitable to measure collisions. Existing works are mostly limited to measure spin noise originated from Zeeman sublevels [24,26,32], where collisional shifts are only on the order of 10^{-2} Hz [7] and challenging to observe. Moreover, although hyperfine frequency shifts are on the order of 100 kHz, existing techniques suffer from a trade-off between bandwidth and spectral resolution. Specifically, the bandwidth is usually below 1 GHz because of limited bandwidths of available balanced detectors and data-acquisition cards (DACs) [31,38,39]. Although some photodetectors and DACs can have gigahertz bandwidth, applications of them are still challenging since they require unrealistically high-speed real-time storage

and large data processing [44,47]. Many ongoing efforts have been recently reported, for example, using ultra-fast pair laser pulses [38] or optical heterodyne [39], but the state-of-the-art resolution is still only a few hundred kilohertz [39].

To address this difficulty, we introduce a frequency down-conversion technique as shown in Fig. 2, where the collision-sensitive spin-noise signal is converted from microwave to radio-frequency range. Specifically, raw spin-noise signals oscillating at $\nu_{mn} + \nu_{\text{shift}}^{mn}$ are multiplied with reference signals at ν_{mn}^{ref} , which are close to ν_{mn} , by a low-pass mixer to reserve low-frequency signals at $\nu_{mn}^{\text{rel}} = |\nu_{mn} - \nu_{mn}^{\text{ref}} + \nu_{\text{shift}}^{mn}|$ [48]. Although ν_{mn} is on the order of 1 GHz, ν_{mn}^{rel} can be about 10 MHz. Therefore, real-time measurement of down-converted spin-noise signals can be achieved with DACs with tens of megahertz bandwidth, significantly reducing the data amount by approximately 99%. The phase noise of reference signals causes the spectral broadening $\gamma_{\text{ref}} \sim 0.1$ Hz [48], which is far smaller than γ_{mn} and thus can be neglected.

Figure 3 shows an example of experimental noise spectra from Rb atoms colliding with N_2 molecules. To simultaneously detect hyperfine transitions of two Rb isotopes, we use the array of two microwave synthesizers to down-convert spin-noise signals. Figure 3(a) shows such a spectrum of natural abundance Rb in zero magnetic field. The blue and red spectra are from colliding ^{85}Rb and ^{87}Rb atoms, yielding hyperfine splittings, i.e., 3035.79 and 6834.83 MHz, respectively. The theoretical hyperfine splittings are 3035.73 and 6834.68 MHz for free ^{85}Rb and ^{87}Rb atoms [49], respectively. A small frequency shift exists between experimental and theoretical values, which is different for two isotopes. The observation of the small shift demonstrates the ability of our technique for measuring collision phenomena. The effective spin dephasing rate is about $\gamma_{mn} \approx 7$ kHz, which is mainly due to the transit time of atoms across the approximately $230\text{-}\mu\text{m}$ beam [24]. In spite of this transit-time broadening, the resolution of our method is still at least 2 orders of magnitude better than existing gigahertz spin-noise techniques [38,39].

The collisional shifts of interhyperfine sublevels are measured. To do this, a small magnetic field is applied. Figures 3(b) and 3(c) show spin-noise spectra in a transverse and longitudinal magnetic field (approximately 76 mG), respectively. In these cases, the zero-field peak splits into resolvable multiplet, corresponding to transitions with $\Delta F = 1$, $\Delta M_F = \pm 1$, and $\Delta M_F = 0$ in turn [32], which is consistent with Eq. (3). Every peak equally shifts about 60 and 150 kHz for ^{85}Rb and ^{87}Rb , respectively, which are equal to those in zero magnetic field. This is because that sublevels within the same hyperfine manifold shift equally, but those in different manifolds shift unequally. Besides, the frequency difference between adjacent peaks is $\Delta\nu_{mn} \approx 71$ (106) kHz for ^{85}Rb (^{87}Rb), which is approximately equal to $\Delta\nu_{mn} \approx 2g_F\mu_BB$. We observe

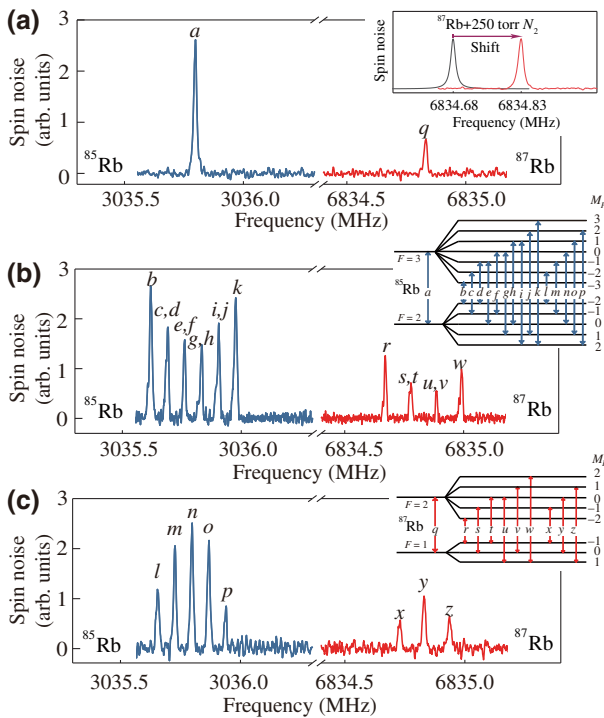


FIG. 3. Collision-sensitive spin-noise experimental spectra. (a) Zero-field spin-noise spectra for ⁸⁵Rb and ⁸⁷Rb hyperfine levels. The inset shows a demonstration of ⁸⁷Rb collision-induced frequency shift. (b),(c) The measured spin-noise spectra in a 76-mG transverse and longitudinal magnetic fields, respectively. The corresponding spin-noise peaks correspond to those transitions between Zeeman sublevels belonging to different hyperfine sublevels (i.e., $\Delta F = 1$, $\Delta M_F = 0, \pm 1$). The insets show the corresponding energy levels and allow interhyperfine transitions of ⁸⁵Rb and ⁸⁷Rb.

no significant collisional shifts of Zeeman sublevels. This verifies that collisional shifts of Zeeman sublevels are significantly smaller than those of interhyperfine sublevels.

We would like to emphasize differences between our technique and traditional spectrum analyzers. Due to no need of high-bandwidth DACs, spectrum analyzers employing swept local oscillators are usually adopted to measure signals at gigahertz range, however they ignore most data [50]. For example, measuring a spectrum with 10 MHz window and 1 kHz resolution effectively uses only approximately 0.01% of data [47]. In contrast, our technique avoids this by fast Fourier transforming of down-converted data in a FPGA [44], realizing 100% data utilization and therefore reducing measurement time by more than 3 orders of magnitude. Moreover, with only one frequency component detected each time, spectrum analyzers can not extract correlations between different frequencies [51,52], which are useful to study many-body interactions in correlated systems [31,37]. To overcome this, we employ multiple reference signals to simultaneously measure signals at corresponding frequencies, as demonstrated in Fig. 3. Besides, spectrum

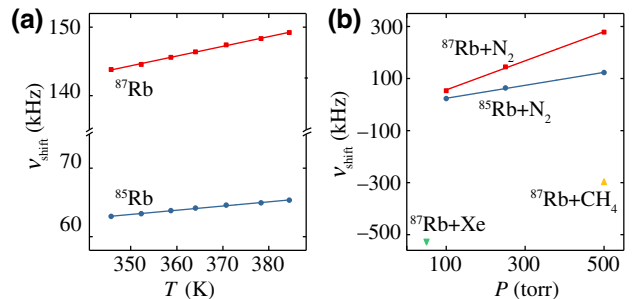


FIG. 4. (a) Collisional shifts of Rb atoms versus vapor temperature in the presence of 250 torr N₂. The shifts linearly increase with the temperature. (b) Collisional shifts of Rb atoms versus vapor pressure at $T_0 = 337$ K. The shifts linearly increase with the pressure. In (a),(b), error bars are within data points.

analyzers are not suitable for studying higher-order correlations that have multitime moments [37,53]. With the capability of real-time measurement, our technique has the potential of measuring higher-order cumulants.

Measurement of collision parameters.—With the use of collision-sensitive spin-noise spectra, collision parameters can be precisely determined. As shown in Fig. 4(a), our experiments are performed in a relatively small temperature range, and collisional shifts are nearly linear to the vapor temperature. In this case, the collisional shift can be expanded to the first order of $(T - T_0)$. According to Eq. (1), the collisional shift is proportional to the number density of inert atoms or molecules, as confirmed by experiments shown in Fig. 4(b). Here we change the number density via changing the pressure of inert atoms or molecules at a constant temperature T_0 . As a result, the collisional shift in Eq. (1) can be approximated as

$$v_{\text{shift}} \approx P_0[\beta + \delta(T - T_0)] + O[(T - T_0)^2], \quad (4)$$

where P_0 and T_0 are the reference vapor pressure and temperature, respectively, and are calibrated through absorption spectra of Rb atoms [48,54]. β is the pressure-dependent coefficient and measured to be 559 Hz/torr and 249 Hz/torr for ⁸⁷Rb-N₂ and ⁸⁵Rb-N₂ pairs, respectively. δ is the temperature-dependent coefficient and measured to be 0.57 Hz/(K torr) and 0.25 Hz/(K torr) for ⁸⁷Rb-N₂ and ⁸⁵Rb-N₂ pairs, respectively. We find the ratio between pressure-dependent or temperature-dependent shifts of two Rb isotopes are 2.28 and 2.24, respectively, which are close to their hyperfine splitting ratio (2.25) [10].

We now consider the intermolecular potential as the Lennard-Jones potential in Eq. (2), which has been widely studied in analyzing gas collisions [6, 42]. Based on Eq. (1), we expand the shift using Eq. (4), and get relations between pressure-dependent coefficient β and temperature-dependent coefficient δ with parameters $\{\epsilon_1, \epsilon_2, \sigma_1, \sigma_2\}$ [48]. Combined with the

other two theoretical formulas, simultaneous analysis of $\beta(\epsilon_1, \epsilon_2, \sigma_1, \sigma_2)$ and $\delta(\epsilon_1, \epsilon_2, \sigma_1, \sigma_2)$ can finally derive the four parameters [48]. Specifically, for the $^{87}\text{Rb}-\text{N}_2$ pair, we obtain the collision diameter $\sigma_1 \approx 4.19 \text{ \AA}$, the well depth $\epsilon_1 \approx 7.6 \text{ meV}$, which are in good agreement with theoretical results [6]. Moreover, we find that collision parameters $\{\epsilon_1, \epsilon_2, \sigma_1, \sigma_2\}$ for $^{85}\text{Rb}-\text{N}_2$ pairs are the same with those of $^{87}\text{Rb}-\text{N}_2$ pairs, yielding that collision parameters are usually independent of the nuclear structure of Rb isotopes.

We also test the feasibility of our technique to investigate ^{87}Rb atoms colliding with different atoms and molecules, for example, CH_4 and Xe. The frequency shifts induced by N_2 with relatively small electric polarizability are positive [see Fig. 1(c)], yielding that the Pauli exclusion is dominant for Rb- N_2 pairs [8]. In contrast, when Rb atoms collide with atoms or molecules that have relatively large electric polarizability [see Fig. 1(b)], such as Xe and CH_4 [see Fig. 4(b)], the van der Waals interaction dominates [8]. Our result clearly shows the dominant potential type for different pairs via the sign of frequency shifts. This suggests a convenient way to analyze the information of inert atoms and molecules, such as atomic or molecular electric polarizability.

Conclusions.—In conclusion, we propose and demonstrate a spin-noise technique that is capable of characterizing collision phenomena in alkali atoms and inert atoms or molecules. In contrast to frequently used scattering approaches that require ultrahigh vacuum systems, our technique *in situ* measures collisions with simple apparatus and ambient conditions but still with high precision. Comparing with traditional hyperfine resonance approaches [6,8,11], our techniques are nonperturbative [24,27,31] and avoid extra heating caused by laser pumping, therefore our technique can be a promising probe of cold and ultracold atomic collisions [34,35]. The present approach can be extended to investigate complicated intermolecular potentials, for example, modified Lennard-Jones potential [5,6] and Buckingham potential [42]. To measure such potentials, we can measure the collision-sensitive spin noise under a large temperature range, then obtain high-order coefficients of T^n term of v_{shift} , and in turn extract the collision parameters. Besides, this noise-based method may also adopt optical heterodyne that enables low-power and small perturbative optical measurement [39,55].

Acknowledgments.—We thank Dmitry Budker, Kaifeng Zhao, Xu Shan, Zhen-Sheng Yuan, and Heng Shen for valuable discussions. This work is supported by National Key Research and Development Program of China (Grant No. 2018YFA0306600), National Natural Science Foundation of China (Grants No. 11661161018, No. 11927811, and No. 12004371), Anhui Initiative in Quantum Information Technologies (Grant No. AHY050000), the Hong Kong RGC/NSFC Joint Research Scheme Project N_CUHK403/16, and USTC Research Funds of the Double First-Class Initiative (Grant No. YD3540002002).

- [1] M. L. Goldberger and K. M. Watson, *Collision Theory* (Dover, New York, 2004).
- [2] W. Xiong, A. Gasparian, H. Gao, D. Dutta, M. Khan-daker, N. Liyanage, E. Pasyuk, C. Peng, X. Bai, and L. Ye *et al.*, A small proton charge radius from an electron–proton scattering experiment, *Nature* **575**, 147 (2019).
- [3] L. Frommhold, *Collision-Induced Absorption in Gases* (Cambridge University Press, London, 2006).
- [4] A. Bartocci, D. Cappelletti, F. Pirani, F. Tarantelli, and L. Belpassi, Intermolecular interaction in the $\text{H}_2\text{S}-\text{H}_2$ complex: Molecular beam scattering experiments and Ab-Initio calculations, *J. Phys. Chem. A* **118**, 6440 (2014).
- [5] T. Karman, M. A. Koenis, A. Banerjee, D. H. Parker, I. E. Gordon, A. van der Avoird, W. J. van der Zande, and G. C. Groenenboom, O_2-O_2 and O_2-N_2 collision-induced absorption mechanisms unravelled, *Nat. Chem.* **10**, 549 (2018).
- [6] L. B. Robinson, Frequency shifts in the hyperfine spectra of alkalis caused by foreign gases, *Phys. Rev.* **117**, 1275 (1960).
- [7] R. M. Herman, Rare-gas-induced g_J shifts in the ground states of alkali atoms, *Phys. Rev.* **175**, 10 (1968).
- [8] R. Bernheim and L. Kohuth, Effects of molecular buffer gases on the cesium hyperfine frequency, *J. Chem. Phys.* **50**, 899 (1969).
- [9] Y. Sortais, S. Bize, C. Nicolas, A. Clairon, C. Salomon, and C. Williams, Cold Collision Frequency Shifts in a ^{87}Rb Atomic Fountain, *Phys. Rev. Lett.* **85**, 3117 (2000).
- [10] D. Budker, L. Hollberg, D. F. Kimball, J. Kitching, S. Pustelny, and V. V. Yashchuk, Microwave transitions and nonlinear magneto-optical rotation in anti-relaxation-coated cells, *Phys. Rev. A* **71**, 012903 (2005).
- [11] E. P. Corsini, T. Karaulanov, M. Balabas, and D. Budker, Hyperfine frequency shift and Zeeman relaxation in alkali-metal-vapor cells with antirelaxation alkene coating, *Phys. Rev. A* **87**, 022901 (2013).
- [12] C. J. Jameson, Gas-phase NMR spectroscopy, *Chem. Rev.* **91**, 1375 (1991).
- [13] D. Budker and M. Romalis, Optical magnetometry, *Nat. Phys.* **3**, 227 (2007).
- [14] M. Jiang, T. Wu, J. W. Blanchard, G. Feng, X. Peng, and D. Budker, Experimental benchmarking of quantum control in zero-field nuclear magnetic resonance, *Sci. Adv.* **4**, eaar6327 (2018).
- [15] M. Jiang, R. P. Frutos, T. Wu, J. W. Blanchard, X. Peng, and D. Budker, Magnetic Gradiometer for the Detection of Zero-To Ultralow-Field Nuclear Magnetic Resonance, *Phys. Rev. Appl.* **11**, 024005 (2019).
- [16] M. Jiang, W. Xu, Q. Li, Z. Wu, D. Suter, and X. Peng, Interference in atomic magnetometry, *Adv. Quantum Technol.* **3**, 2000078 (2020).
- [17] M. Jiang, H. Su, Z. Wu, X. Peng, and D. Budker, Floquet maser, *Sci. Adv.* **7**, eabe0719 (2021).
- [18] M. Jing, Y. Hu, J. Ma, H. Zhang, L. Zhang, L. Xiao, and S. Jia, Atomic superheterodyne receiver based on microwave-dressed Rydberg spectroscopy, *Nat. Phys.* **16**, 911 (2020).
- [19] H. Margenau, P. Fontana, and L. Klein, Frequency shifts in hyperfine splitting of alkalis caused by foreign gases, *Phys. Rev.* **115**, 87 (1959).
- [20] M. D. Rotondaro and G. P. Perram, Collisional broadening and shift of the rubidium D1 and D2 lines ($5^2\text{S}_{1/2} \rightarrow$

- $5^2P_{1/2}$, $5^2P_{3/2}$) by rare gases, H₂, D₂, N₂, CH₄ and CF₄, *J. Quant. Spectrosc. Ra.* **57**, 497 (1997).
- [21] J. Kong, R. Jiménez-Martínez, C. Troullinou, V. G. Lucivero, G. Tóth, and M. W. Mitchell, Measurement-induced, spatially-extended entanglement in a hot, strongly-interacting atomic system, *Nat. Commun.* **11**, 1 (2020).
- [22] K. Mouloudakis and I. Kominis, Spin-exchange collisions in hot vapors creating and sustaining bipartite entanglement, *Phys. Rev. A* **103**, L010401 (2021).
- [23] E. Aleksandrov and V. Zapasskii, Magnetic resonance in the faraday-rotation noise spectrum, *Zh. Eksp. Teor. Fiz.* **81**, 132 (1981).
- [24] S. Crooker, D. Rickel, A. Balatsky, and D. Smith, Spectroscopy of spontaneous spin noise as a probe of spin dynamics and magnetic resonance, *Nature* **431**, 49 (2004).
- [25] M. Oestreich, M. Römer, R. J. Haug, and D. Hägele, Spin Noise Spectroscopy in GaAs, *Phys. Rev. Lett.* **95**, 216603 (2005).
- [26] F. Li, Y. V. Pershin, V. A. Slipko, and N. A. Sinitsyn, Nonequilibrium Spin Noise Spectroscopy, *Phys. Rev. Lett.* **111**, 067201 (2013).
- [27] V. S. Zapasskii, A. Greilich, S. A. Crooker, Y. Li, G. G. Kozlov, D. R. Yakovlev, D. Reuter, A. D. Wieck, and M. Bayer, Optical spectroscopy of spin noise, *Phys. Rev. Lett.* **110**, 176601 (2013).
- [28] P. Glesenapp, N. Sinitsyn, L. Yang, D. Rickel, D. Roy, A. Greilich, M. Bayer, and S. Crooker, Spin Noise Spectroscopy beyond Thermal Equilibrium and Linear Response, *Phys. Rev. Lett.* **113**, 156601 (2014).
- [29] S. Cronenberger, D. Scalbert, D. Ferrand, H. Boukari, and J. Cibert, Atomic-like spin noise in solid-state demonstrated with manganese in cadmium telluride, *Nat. Commun.* **6**, 1 (2015).
- [30] L. Yang, P. Glesenapp, A. Greilich, D. Reuter, A. Wieck, D. Yakovlev, M. Bayer, and S. Crooker, Two-colour spin noise spectroscopy and fluctuation correlations reveal homogeneous linewidths within quantum-dot ensembles, *Nat. Commun.* **5**, 1 (2014).
- [31] N. A. Sinitsyn and Y. V. Pershin, The theory of spin noise spectroscopy: A review, *Rep. Prog. Phys.* **79**, 106501 (2016).
- [32] Y. Tang, Y. Wen, L. Cai, and K. Zhao, Spin-noise spectrum of hot vapor atoms in an anti-relaxation-coated cell, *Phys. Rev. A* **101**, 013821 (2020).
- [33] S. Cronenberger, C. Abbas, D. Scalbert, and H. Boukari, Spatiotemporal Spin Noise Spectroscopy, *Phys. Rev. Lett.* **123**, 017401 (2019).
- [34] K. Eckert, O. Romero-Isart, M. Rodriguez, M. Lewenstein, E. S. Polzik, and A. Sanpera, Quantum non-demolition detection of strongly correlated systems, *Nat. Phys.* **4**, 50 (2008).
- [35] G. M. Bruun, B. M. Andersen, E. Demler, and A. S. Sørensen, Probing Spatial Spin Correlations of Ultracold Gases by Quantum Noise Spectroscopy, *Phys. Rev. Lett.* **102**, 030401 (2009).
- [36] S.-W. Chen and R.-B. Liu, Faraday rotation echo spectroscopy and detection of quantum fluctuations, *Sci. Rep.* **4**, 4695 (2014).
- [37] F. Li and N. Sinitsyn, Universality in Higher Order Spin Noise Spectroscopy, *Phys. Rev. Lett.* **116**, 026601 (2016).
- [38] F. Berski, H. Kuhn, J. G. Lonnemann, J. Hübner, and M. Oestreich, Ultrahigh Bandwidth Spin Noise Spectroscopy: Detection of Large g-factor Fluctuations in Highly-N-doped GaAs, *Phys. Rev. Lett.* **111**, 186602 (2013).
- [39] S. Cronenberger and D. Scalbert, Quantum limited heterodyne detection of spin noise, *Rev. Sci. Instrum.* **87**, 093111 (2016).
- [40] A. Kumar, T.-Y. Wu, F. Giraldo, and D. S. Weiss, Sorting ultracold atoms in a three-dimensional optical lattice in a realization of Maxwell's demon, *Nature* **561**, 83 (2018).
- [41] D. Smirnov and K. Kavokin, Optical resonance shift spin-noise spectroscopy, *Phys. Rev. B* **101**, 235416 (2020).
- [42] I. G. Kaplan, *Intermolecular Interactions: Physical Picture, Computational Methods and Model Potentials* (John Wiley & Sons, New York, 2006).
- [43] M. E. Rose, *Elementary Theory of Angular Momentum* (Dover, New York, 1995).
- [44] Y. Tong, L. Wang, W.-Z. Zhang, M.-D. Zhu, X. Qin, M. Jiang, X. Rong, and J. Du, A high performance fast-fourier-transform spectrum analyzer for measuring spin noise spectrums, *Chin. Phys. B* (2020).
- [45] G. Katsoprinakis, A. Dellis, and I. Kominis, Measurement of transverse spin-relaxation rates in a rubidium vapor by use of spin-noise spectroscopy, *Phys. Rev. A* **75**, 042502 (2007).
- [46] R. Kubo, The fluctuation-dissipation theorem, *Rep. Prog. Phys.* **29**, 255 (1966).
- [47] S. Crooker, J. Brandt, C. Sandfort, A. Greilich, D. Yakovlev, D. Reuter, A. Wieck, and M. Bayer, Spin Noise of Electrons and Holes in Self-Assembled Quantum Dots, *Phys. Rev. Lett.* **104**, 036601 (2010).
- [48] See Supplemental Material at <http://link.aps.org/supplemental/10.1103/PhysRevApplied.17.L011001> for calibrations of the pressure and the temperature of the vapor cell and determination of collision parameters.
- [49] D. A. Steck, Rubidium 87 D Line Data (2001).
- [50] M. Römer, J. Hübner, and M. Oestreich, Spin noise spectroscopy in semiconductors, *Rev. Sci. Instrum.* **78**, 103903 (2007).
- [51] A. Dellis, M. Loulakis, and I. Kominis, Spin-noise correlations and spin-noise exchange driven by low-field spin-exchange collisions, *Phys. Rev. A* **90**, 032705 (2014).
- [52] K. Mouloudakis, M. Loulakis, and I. Kominis, Quantum trajectories in spin-exchange collisions reveal the nature of spin-noise correlations in multispecies alkali-metal vapors, *Phys. Rev. Res.* **1**, 033017 (2019).
- [53] P. Wang, C. Chen, X. Peng, J. Wrachtrup, and R.-B. Liu, Characterization of Arbitrary-Order Correlations in Quantum Baths by Weak Measurement, *Phys. Rev. Lett.* **123**, 050603 (2019).
- [54] C. Alcock, V. Itkin, and M. Horrigan, Vapour pressure equations for the metallic elements: 298–2500 K, *Can. Metall. Quart.* **23**, 309 (1984).
- [55] P. Sterin, J. Wiegand, J. Hübner, and M. Oestreich, Optical Amplification of Spin Noise Spectroscopy via Homodyne Detection, *Phys. Rev. Appl.* **9**, 034003 (2018).